Available online at www.sciencedirect.com

ScienceDirect

Proceedings of the Combustion Institute 000 (2020) 1–8

Proceedings of the Combustion Institute

www.elsevier.com/locate/proci

Surface morphology and inner fractal cutoff scale of spherical turbulent premixed flames in decaying isotropic turbulence

Tejas Kulkarni, Fabrizio Bisetti*

Department of Aerospace Engineering and Engineering Mechanics, University of Texas at Austin, Austin, TX 78712, USA

Received 7 November 2019; accepted 8 June 2020
Available online xxx

Abstract

The surface of turbulent premixed flames is fractal within a finite range of scales and the fractal dimension and inner cutoff scale are key components of fractal turbulent combustion closures. In such closures, the estimate for the surface area is sensitive to the value of the inner fractal cutoff scale, whose modeling remains unclear and for which both experimental and numerical contradictory evidence exists. In this work, we analyze data from six direct numerical simulations of spherically expanding turbulent premixed flames at varying Reynolds and Karlovitz numbers. The flames propagate in decaying isotropic turbulence and fall in the flamelet regime. Past an initial transient, we find that the fractal dimension reaches an asymptotic value between 2.3 and 2.4 in good agreement with previous results at similar conditions. A minor dependence of the fractal dimension on the Reynolds and Karlovitz numbers is observed and explained by the relatively low values of the Reynolds number and narrow inertial and fractal ranges. The inner fractal cutoff scale Δ^* is found to scale as $\Delta^*/l \sim \mathrm{Re}_\lambda^{-1.14}$, where l is the integral scale of turbulence and Re_λ is the Reynolds number based on the Taylor micro-scale computed in the turbulence on the reactants' side. The scaling is robust and insensitive to the Karlovitz number over the range of values considered in this study. An important implication is that the ratio Δ^*/η grows with Reynolds number (η is the Kolmogorov scale), albeit at a rather slow rate that may explain the widespread observation that $4 \leq \Delta^*/\eta \leq 10$. This suggests that Δ^*, although smaller than λ, is not a dissipative length scale for the flame surface and scaled solely by η. Finally, a dissipative threshold scale that remains constant once normalized by η is identified.

Keywords: Fractal morphology; Turbulent premixed combustion; Direct numerical simulation; Inner fractal cutoff scale; Flame surface

* Corresponding author.
E-mail address: fbisetti@utexas.edu (F. Bisetti).

https://doi.org/10.1016/j.proci.2020.06.117
1540-7489 © 2020 Published by Elsevier Inc. on behalf of The Combustion Institute.

1. Introduction

The surface of a turbulent premixed flame is wrinkled by turbulence over a range of scales and displays a fractal behavior in a subset of this range [1–3]. Within the fractal range, the area of the flame surface depends on the size of the measurement scale according to a power law with an exponent related to the *fractal dimension*. As the measurement scale decreases, the measured area of the fractal surface increases. At scales smaller than these in the fractal range, the area becomes independent of the measurement scale and equal to the area of the flame surface. The measurement scale where this smooth transition occurs is the *inner fractal cutoff scale*.

The cutoff scale and the fractal dimension are two inputs required by fractal models in turbulent premixed combustion closures [4]. Fractal models extrapolate the area measured at a resolved scale, typically equal to the spatial resolution of the computational mesh, to the inner cutoff scale, where the area is equal to the flame surface area. Despite their robust theoretical foundation, uncertainties in either the fractal dimension or the inner fractal cutoff scale compromise the models' accuracy.

The fractal dimension of the surface of turbulent premixed flames is observed to lie in the range 2.3 to 2.7 [5,6]. In the corrugated flamelet limit, theoretical considerations suggest $7/3 = 2.33$ [2], consistent with Kolmogorov's -5/3 scaling and isosurfaces in isothermal turbulent flows [3]. Others have shown that high Karlovitz numbers lead to an increase in the fractal dimension and provided theoretical arguments in support of $8/3 = 2.67$ [5]. In practice, the fractal dimension of turbulent flames varies in space and time, at least during the early stages of flame development, possibly contributing to the relatively broad range of values reported.

The estimate of the inner fractal cutoff scale remains even more controversial. While it is accepted that dissipation is responsible for suppressing the fractal morphology of surfaces at the small scales, it is unclear if the inner cutoff scale is simply a multiple of η by a constant factor and independent of Reynolds and Karlovitz numbers or not. Fractal cutoff scale values between 4η and 10η are consistently reported, but proposed models that scale the cutoff scale with the flame thermal thickness or the Kolmogorov scale are unable to explain the scatter in the data convincingly [5,6].

In this work, we investigate the fractal properties of spherical turbulent premixed flames burning in decaying isotropic turbulence. The configuration presents an opportunity to a study the development of a smooth spherical kernel of burnt gases as it evolves into a wrinkled turbulent premixed flame and allows for the investigation of the dependence of the fractal properties of turbulent flames over a wide range of Reynolds and Karlovitz numbers with emphasis on the scaling of the inner fractal cutoff scale from these two dimensionless groups.

2. Governing equations, models, and methods

The evolution of the flame is described by the multi-component reactive Navier–Stokes equations, which are solved in the low Mach number limit. Heat and mass fluxes are closed by the Hirschfelder-Curtiss model with mixture-average transport coefficients [7–9]. Reactions are modeled by a finite rate skeletal mechanism consisting of 16 species and 73 elementary reactions for lean methane/air combustion at 800 K and 4 atm. The mechanism was reduced from GRI Mech 3.0 and validated for use in simulations of turbulent combustion [10].

The equations are discretized on a staggered finite difference homogeneous Cartesian mesh and solved with the massively parallel solver "NGA" [11]. All spatial discretizations are second and third order accurate for the momentum and reactive scalar fields, respectively. Coupling between pressure and momentum is enforced by a pressure-correction approach. Time integration is explicit for the convective terms and implicit for the viscous and diffusive terms. Chemical sources are integrated in time separately from transport with first order Lie-splitting. Third-party libraries are used for the solution of the variable coefficients Poisson pressure equation (Hypre) and the system of ordinary differential equations for chemical reactions (CVODE) at each mesh point. More details are available in Refs. [8,9].

The simulations are performed in a cubic domain with periodic boundary conditions. The mesh spacing is $\Delta x = \Delta y = \Delta z = h$ and such that $h/\eta \leq 0.5$ and $\delta_L/h \geq 5.5$ at all times, where η is the Kolmogorov length scale and δ_L is the thermal thickness of the laminar flame. Similarly, the time step size is such that $\tau_\eta/\Delta t \geq 20$, where τ_η is the Kolmogorov time scale. The adequacy of spatial and temporal resolution of turbulence and flame front were previously demonstrated for turbulent premixed jet flames under identical thermo-chemical conditions by performing extensive numerical convergence tests [9].

3. Configurations and overview

The configuration consist in a closed cubic domain, initially filled with a reactive mixture of lean methane/air (equivalence ratio of 0.7) at 800 K and 4 atm. The initial turbulent velocity field is obtained with auxiliary simulations of statistically stationary homogeneous isotropic turbulence, which are patched together and scaled appropriately in order to obtain the desired turbulence parameters and domain size. Once the velocity field is prescribed, a

Please cite this article as: T. Kulkarni and F. Bisetti, Surface morphology and inner fractal cutoff scale of spherical turbulent premixed flames in decaying isotropic turbulence, Proceedings of the Combustion Institute, https://doi.org/10.1016/j.proci.2020.06.117

Table 1
Simulation parameters: $\mathrm{Re}_\lambda = u'\lambda/\nu$, and $\mathrm{Ka} = \tau_L/\tau_\eta$. Here u' is the velocity fluctuation, λ the Taylor microscale, ν the kinematic viscosity of the reactants, $\tau_0 = k_0/\epsilon_0$ is the eddy turnover time at the onset of the simulation with k_0 indicating the turbulent kinetic energy and ϵ_0 its mean rate of dissipation, and τ_η the Kolmogorov time scale. The ratio of maximum flame radius $R_{\max}$ to the domain size L is also listed. Laminar flame speed $S_L = 1.0$ m/s, thermal thickness $\delta_L = 0.11$ mm, and flame time $\tau_L = \delta_L/S_L = 0.11$ ms are the same across simulations and do not vary appreciably in time.

	R1K1	R2K1	R2a	R3K1	R3K2	R3K3
N^3	512^3	1024^3	1024^3	2048^3	1024^3	1024^3
u/S_L	7.3	8.6	7.3	9.8	14.7	19.7
l/δ_L	3.3	5.2	6.3	7.8	4.9	3.9
Re_λ	43	58	58	77	77	77
Ka	25	25	18	25	58	100
$2R_{\max}/L$	0.53	0.44	0.57	0.33	0.46	0.37

spherical kernel of burnt gases is placed at the center of the domain. The ensuing spherical turbulent premixed flame propagates outward and grows in size as turbulence decays.

The configuration is advantageous for this study as it is amenable to direct experimental validation and retains the complexity of a real flow with two inhomogeneous directions (time and radial coordinates). At the same time, the temporal evolution of the mean velocity field and fluctuations in this configuration are very well understood, which simplifies the analysis. Although the pressure increases because the domain is closed, the increase is minor on the account of the large domain size and inconsequential to the analysis.

The simulations and analysis are conducted for six spherical turbulent premixed flames with different initial conditions (Table 1). Altogether, the configurations allow to investigate the effect of Reynolds number (at constant Ka) and of Karlovitz number (at constant Re_λ) on flame morphology. More details of the simulation database are provided in [8,12], along with an analysis of the flame surface area, surface density function, and turbulent burning rates.

In order to avoid the effects of periodic boundaries, only the data for which the linear size of the flame is less than 50% of the domain are considered ($2R_{\max}/L \lesssim 0.5$). Unless otherwise noted, all turbulence parameters are evaluated in the reactants.

Representative three-dimensional renders of the flame surface $C(\mathbf{x}, t) = c^* = 0.73$ are shown in Fig. 1a. In this work, C is defined based on the mass fraction of molecular oxygen and the value $c^* = 0.73$ identifies peak heat release rate and the flame's reaction zone. No appreciable changes to the analysis were observed for values of c^* within the range 0.1 to 0.9. As shown, the flame surface is wrinkled over a multitude of scales and folded by turbulence with most regions being flat or characterized by a slight curvature. Patches of high curvature present as sharp cylindrical folds.

Turbulence decays in time and the appropriate time coordinate is the logarithmic time $s = \log(1 + t/m\tau_0)$, where m is the exponent that governs the exponential decay of turbulent kinetic energy as $k/k_0 = (1 + t/m\tau_0)^{-m}$. We find $m = 1.55$ for all flames, so that comparisons across flames are conducted at the same values of t/τ_0 (or s). Isothermal simulations of decaying turbulence confirmed that the statistics of turbulence in the reactants are not affected by the presence of the turbulent flame nor by the minor increase in pressure.

The mean flame radius is $R = R(t)$ and the turbulent flame brush is $\delta = \delta(t) = \sqrt{2\pi}\sigma$, where σ is the standard deviation of the flame distance from the origin, and its evolution is shown in Fig. 1c. When scaled by the instantaneous value of the integral scale $l = u'^3/\epsilon$ and plotted versus t/τ_0, the temporal evolution of δ/l is self-similar with a minor dependence on Re_λ. This conclusion is supported by the fact that δ/l is nearly the same for flames with the same Reynolds number: R2K1 and R2a ($\mathrm{Re}_\lambda = 58$) and R3K1, R3K2, and R3K3 ($\mathrm{Re}_\lambda = 77$). Differences appear at later times across all flames: $\pm 35\%$ of the mean at $t/\tau_0 = 3.6$.

4. Results

The first step of the analysis consists in extracting a triangle mesh of the iso-surface $C(\mathbf{x}, t) = c^*$ from the discrete solution C^n_{ijk} via the marching cubes algorithm [13]. A dual mesh of cubic volumes, each of side h and centered at (x_i, y_j, z_k), is generated also, together with a corresponding voxel grid, whereby each voxel is set equal to one if the corresponding dual mesh volume contains the triangle mesh and zero otherwise. This second step provides a digitized representation of the flame surface on a voxel grid consistent with the finite difference mesh. The voxel values are stored in a three-dimensional matrix of zeros and ones. Third, the box-counting algorithm [14] is used on the voxel grid to characterize the morphology of the digitized surface by finding N_s, defined as the number of boxes of integer size 2^s ($s = 0, 1, \ldots$) required to cover the set of unit voxels. Because

Please cite this article as: T. Kulkarni and F. Bisetti, Surface morphology and inner fractal cutoff scale of spherical turbulent premixed flames in decaying isotropic turbulence, Proceedings of the Combustion Institute, https://doi.org/10.1016/j.proci.2020.06.117

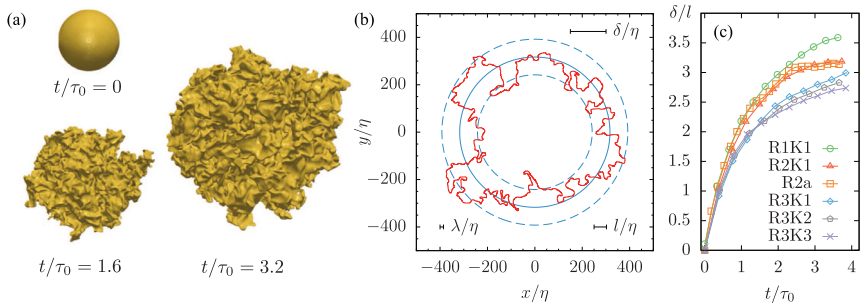

Fig. 1. (a) Turbulent flame R3K1 represented by iso-surface $C(\mathbf{x}, t) = c^* = 0.73$. (b) Iso-contour $C(\mathbf{x}, t) = c^*$ at $t/\tau_0 = 3.2$ on a plane with flame radius R (solid blue line) and $R \pm \delta/2$ (dashed blue line). Only a small portion of the domain is shown. (c) Turbulent flame brush δ/l versus t/τ_0.

box s corresponds to a cube with dimensional side $2^s h$, the procedure returns box counts $N = N(\Delta)$ at increasing measurement scale $\Delta = h, 2h, 4h, \ldots$.

The three steps above are performed multiple times for each discrete field C^n_{ijk}, rotating the finite difference mesh by angles chosen at random and interpolating C^n_{ijk} onto the rotated mesh with a cubic interpolant prior to data reduction. The box counts $N(\Delta)$ at scale Δ are averaged over 100 random rotations.

The entire process, including rotations, is performed $Q + 1$ times starting from interpolated discrete scalar fields $(C^n_{ijk})^q$, each new field obtained by interpolating the discrete solution from the primitive mesh with spacing h onto a mesh with larger spacing $\alpha^q h$, where $\alpha = 2^{1/(Q+1)}$ and $q = 0, \ldots, Q$ ($Q = 3$ in this work). Interpolation onto coarser meshes was found to be inconsequential to the triangle mesh generated by the marching cubes algorithm because the coarsest mesh of spacing $2^{3/4}h$ is sufficiently resolved. This approach allows for box counts at scales other than the primitive set.

The box counts are used to characterize the morphology of the flame surface and to infer the Minkowski–Bouligand (or box-counting) fractal dimension [14] as follows. The quantity

$$A_\Delta = C_1 N \Delta^2 \tag{1}$$

is defined as the *flame surface area measured at scale* Δ and C_1 is a dimensionless constant. If the surface is fractal, the box counts follow a power law $N = C_2 \Delta^{-D_3}$, where C_2 is a dimensional constant, and $D_3 \geq 2$ is the fractal dimension of the surface embedded in three dimensions. In such case, the area at scale Δ follows a power law $A_\Delta = C_1 C_2 \Delta^{2-D_3} = C_3 \Delta^{2-D_3}$ ($C_3 = C_1 C_2$). Because a flame surface is not fractal at all measurement scales, the logarithmic derivative of the box counts N with respect to Δ

$$\xi = \xi(\Delta) = -\frac{d \log N(\Delta)}{d \log \Delta} \tag{2}$$

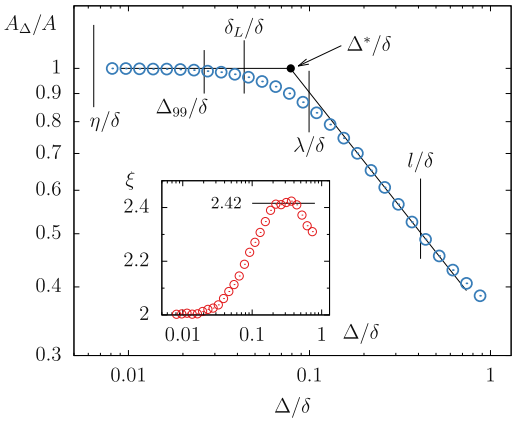

Fig. 2. A_Δ/A versus Δ/δ (Eq. (1) with $C_1 = 2/3$), where δ is the turbulent brush thickness and A is the flame surface area. Data for R3K1 at $t/\tau_0 = 2$. See the commentary for a definition of all scales marked by vertical lines. The solid line corresponds to the power law fit $N \sim \Delta^{-D_3}$ with $D_3 = 2.42$ in the range $0.2 \leq \Delta/\delta \leq 0.5$. The inset shows ξ (Eq. (2)) and the horizontal line marks the plateau associated with fractal morphology with $D_3 = 2.42$.

represents the *local* fractal dimension at scale Δ. Should ξ be constant over a finite range of measurement scales, the surface displays fractal morphology with fractal dimension $D_3 = \xi$ within that range.

Fig. 2 shows A_Δ/A in Eq. (1) versus the normalized measurement scale Δ/δ, where δ is the turbulent brush thickness, $C_1 = 2/3$, and A is the area of the flame surface. The inset in Fig. 2 shows the logarithmic derivative $\xi = -d \log N / d \log \Delta$ evaluated with a centered finite difference formula.

From Fig. 2, it is apparent that A_Δ increases as Δ decreases, eventually reaching a constant at the smallest values of the measurement scale. In this limit, the value taken by A_Δ is equal to the flame surface area A, indicating that the flame surface is *topologically smooth* [14] at the smallest scale

Please cite this article as: T. Kulkarni and F. Bisetti, Surface morphology and inner fractal cutoff scale of spherical turbulent premixed flames in decaying isotropic turbulence, Proceedings of the Combustion Institute, https://doi.org/10.1016/j.proci.2020.06.117

considered. Further, $\xi \to 2$ as $\Delta \to 0$, consistent with a smooth surface. As Δ increases, ξ increases also, reaching a plateau where it is maximum. In the range $0.2 \leq \Delta/\delta \leq 0.5$, $\xi \approx const$ and the box counts display a power law dependence as $N \sim \Delta^{-D_3}$ with $D_3 = 2.42$, consistent with fractal morphology and power law $A_\Delta/A \sim (\Delta/\delta)^{2-D_3}$. The range where N and Δ are related by a power law is rather narrow. This is due to the limited range of scales involved in the deformation of the flame surface at the low to moderate Re_λ afforded by the simulations.

The choice of the brush thickness δ as a normalizing length is consistent with the fact that the flame surface may not display fractal properties at scales larger than the turbulent brush, which bounds the turbulent flame statistically. This choice is common for fractal interfaces (e.g. see de Silva et. al. [15]) as the measurement scale cannot possibly be larger than the brush. Furthermore, the fractal character of a surface is defined for a volume filled uniformly (in a statistical sense) by a wrinkled surface [1]. Note that $\Delta > \delta/2$ brings a sudden drop in ξ (see inset in Fig. 2), so that $\delta/2$ is taken to represent the *outer fractal cutoff scale* [1] for spherical turbulent premixed flames.

The transition between fractal morphology as described by a power law to a topologically smooth surface is not abrupt, rather it occurs over a range of scales. The intersection of the horizontal $A_\Delta/A = 1$ and the power law identifies the *inner fractal cutoff scale* Δ^* [1,5,6]. Here, an additional scale is defined such that $A_\Delta(\Delta_{99})/A = 0.99$, i.e. the measurement scale for which 99% of the flame surface area is accounted for. For reasons that will become clearer later, Δ_{99} is termed the *dissipative threshold scale*.

In Fig. 2, the following length scales are also shown: $\eta < \Delta_{99} < \delta_L < \Delta^* < \lambda < l < \delta$, where δ is the brush thickness, l the integral length scale, λ the Taylor micro-scale, δ_L the thermal thickness of the laminar flame, and η the Kolmogorov length scale. Their ordering and significance are addressed later.

Fig. 3 shows the evolution of the fractal dimension D_3 for all flames. The Reynolds and Karlovitz numbers decrease in time as shown in Fig. 3b and Fig. 3c, respectively. By design (see Table 1), flames R1K1, R2K1, and R3K1 share the exact same temporal evolution of $\mathrm{Ka} = \mathrm{Ka}(t/\tau_0)$, while flames R3K1, R3K2, and R3K3 share the same evolution of $\mathrm{Re}_\lambda = \mathrm{Re}_\lambda(t/\tau_0)$ and so do flames R2a and R2K1. Flames R1K1 and R2a share the same evolution of u'/S_L (not shown). Although neither Re_λ nor Ka are constant in time, their values across simulations are scaled by a factor that does not vary during the decay of turbulence.

As shown, D_3 grows rapidly, reaching a plateau for $t/\tau_0 > 2$ in all flames. One notable exception is flame R3K3, for which the fractal dimension keeps increasing, albeit at a much lower rate (in units of τ_0). For R3K1, D_3 peaks before decreasing slightly

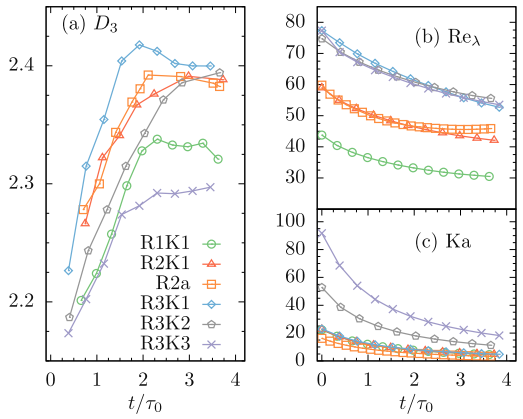

Fig. 3. (a) Fractal dimension D_3 versus time t/τ_0 for all flames. Temporal evolution of (b) Re_λ, and (c) Ka.

towards its asymptotic value. Such early and rapid increase in the fractal dimension is consistent with the flames evolving from smooth spherical kernels of burnt gases. Time is required for the flame radius R and its brush δ to grow and for the flame's surface to attain fractal morphology. It is reasonable to expect that the fractal range may develop if and only if the ratio δ/η is sufficiently large, as δ is an upper cutoff and η bounds from below the size of turbulent motions.

The asymptotic value of the fractal dimension falls in the range 2.32 to 2.42 and these values are consistent with the fractal dimension of turbulent premixed flames in the flamelet regime [2] as well as with the theory and experiments on constant property surfaces in isothermal turbulent flows. In both cases, theoretical arguments support the value of $7/3 = 2.33$ [2,3]. Chatakonda et al. [5] have reported much higher values of the fractal dimension ($2.6 \leq D_3 \leq 2.7$) of low Damköhler, high Karlovitz, and high Reynolds number turbulent premixed flames, consistent with their theoretical estimate of $8/3 = 2.67$.

The data in Fig. 3a allow to conclude the following. First, the higher the Reynolds number (at constant Ka), the higher the value of the fractal dimension throughout the evolution of the flame (R1K1, R2K1, and R3K1). Because the value of D_3 in flames R3K1 and R2K1 are rather similar ($D_3 \approx 2.4$) compared to its lower value in flame R1K1 ($D_3 \approx 2.3$), the fractal dimension appears to be converging to a value independent of the Reynolds number provided that Re_λ is sufficiently large. The value $D_3 = 2.4$ seems plausible and more consistent with values reported in the literature [6]. Second, varying u'/S_L (at constant Re_λ) does not change the evolution of D_3 at low values of Ka (R2K1 and R2a). Conversely, varying Re_λ (at constant u'/S_L and low values of Ka) does change D_3

Please cite this article as: T. Kulkarni and F. Bisetti, Surface morphology and inner fractal cutoff scale of spherical turbulent premixed flames in decaying isotropic turbulence, Proceedings of the Combustion Institute, https://doi.org/10.1016/j.proci.2020.06.117

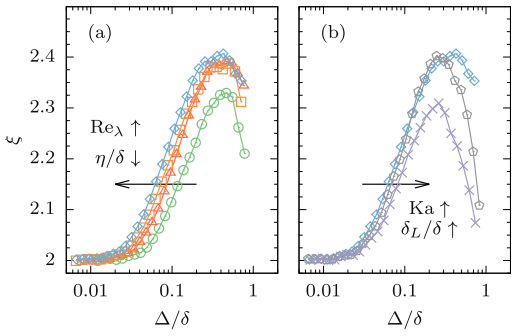

Fig. 4. Logarithmic derivative ξ (Eq. (2)) for all simulations at $t/\tau_0 = 3.6$: (a) constant Ka and varying Re_λ (with the exception of R2a, for which Ka is slightly lower), and (b) constant Re_λ and varying Ka. Symbols are as in Fig. 3.

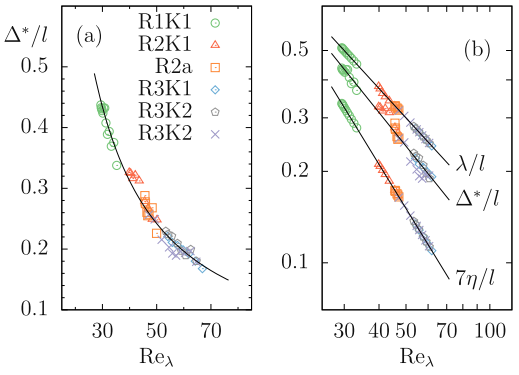

Fig. 5. (a) Inner fractal cutoff scale Δ^*/l versus Re_λ (line is power law fit). (b) Data and power law fits $C\mathrm{Re}_\lambda^\alpha$ (lines): $7\eta/l$ ($\alpha = -1.500$ and $C = 7 \times 7.6159$), λ/l ($\alpha = -1.000$ and $C = 15$), and Δ^*/l ($\alpha = -1.140$, $C = 21.18978$). Data for $t/\tau_0 \geq 1$ are fit and shown.

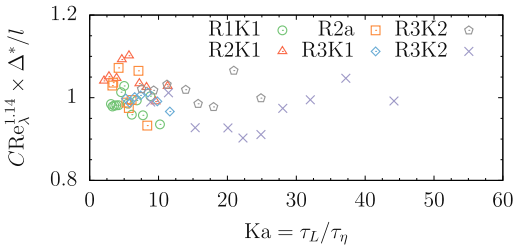

Fig. 6. Inner fractal cutoff scale Δ^*/l compensated by the proposed Reynolds scaling ($C = 0.047193$) and plotted versus Ka for $t/\tau_0 \geq 1$.

considerably (R1K1 and R2a). Third, higher values of Ka correlate with lower values of D_3 during the flame's development, although flames R3K1 (Ka = 25) and R3K2 (Ka = 58) asymptote to the same value of the fractal dimension D_3. Conversely, flame R3K3 (Ka = 100) experiences high values of Ka throughout its evolution and has lower values of D_3.

We postulate that the dependence of D_3 on Re_λ and Ka is due to a narrow inertial range and not a fundamental property of turbulent premixed flames in the flamelet regime. Recall that turbulence theory relates the fractal morphology of interfaces in turbulent flows to the multi-scale nature of turbulence in the inertial range, so that, barring other effects, the fractal dimension is tied to the universal $-5/3$ Kolmogorov scaling [3].

The data in Fig. 4 shows the effect of Re_λ and Ka on the logarithmic derivative ξ. Recall that for the flame to exhibit fractal morphology, ξ should admit a plateau over a sufficiently wide range of measurement scales. As the Reynolds number decreases at constant Ka (Fig. 4a), η/δ increases, delaying the increase of ξ with Δ/δ and suppressing the maximum value attained by ξ, i.e. the fractal dimension. As Ka increases at constant Re_λ (Fig. 4b), a similar shift and suppression of ξ occurs, this time due to increasing laminar flame thickness δ_L/δ at constant η/δ. At low Reynolds numbers, the low degree of separation between η and δ, which was shown to be $\propto l$, exacerbates these effects.

A much debated issue pertains to the scaling of the inner fractal cutoff scale Δ^*, which is often assumed to be a multiple of η or of the thermal flame thickness δ_L. Dependence of the ratio Δ^*/δ_L on the Karlovitz number has long been postulated, although the proposed models are unable to explain the very broad scatter, often across orders of magnitude, in the data [6]. Other authors report $4 \leq \Delta^*/\eta \leq 10$ without any clear dependence on turbulence parameters and Karlovitz number [5,16].

Fig. 5 shows the ratio Δ^*/l versus Reynolds number. On the same plot, 7η, a multiple of the Kolmogorov scale consistent with previously reported values of Δ^* [16], and the Taylor micro-scale λ are shown also. Both $\eta/l \sim \mathrm{Re}_\lambda^{-1.5}$ and $\lambda/l \sim \mathrm{Re}_\lambda^{-1}$ follow the expected scaling with the instantaneous value of Re_λ. Across all simulations and at all times, Δ^* lies between the Taylor micro-scale and the Kolmogorov scale. Most importantly, once normalized by l, the power law scaling $\Delta^*/l \sim \mathrm{Re}_\lambda^{-1.14}$ is rather convincing, especially because it holds in time, across simulations, and with varying Karlovitz number also (R3K1, R3K2, and R3K3).

There exist some residual scatter, illustrated in Fig. 6, where Δ^*/l is compensated by the Re_λ scaling and plotted versus Ka. It appears that variations around unity are small ($\pm 10\%$) and do not correlate with Ka.

The scaling of Δ^*/l implies that $\Delta^*/\eta \sim \mathrm{Re}_\lambda^{0.36}$, i.e. the ratio Δ^*/η increases with Re_λ. Thus, our data do not support the notion that Δ^* is greater than η by a constant factor, *independent* of the Reynolds number. The fact that the exponent of the power law is rather small (0.36) may explain the observation that $\Delta^* \approx 4 - 10\eta$ across multiple studies as

Please cite this article as: T. Kulkarni and F. Bisetti, Surface morphology and inner fractal cutoff scale of spherical turbulent premixed flames in decaying isotropic turbulence, Proceedings of the Combustion Institute, https://doi.org/10.1016/j.proci.2020.06.117

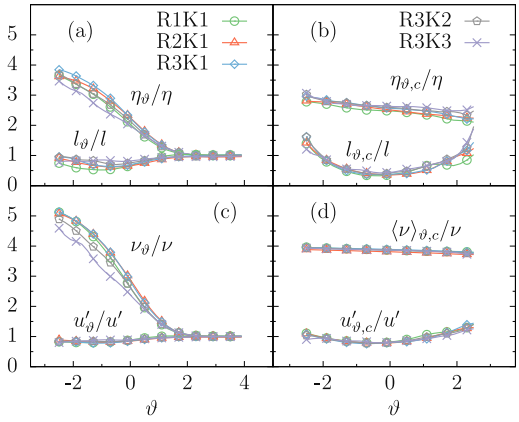

Fig. 7. (a,b) Kolmogorov scale η and integral scale l and (c,d) mean kinematic viscosity $\langle\nu\rangle$ and velocity fluctuation u' computed at the normalized radial coordinate $\vartheta = (r - R)/\sigma$ and normalized by their respective values in the reactants, which depend on time. Subscript c indicates that the statistics are conditioned on $C = c^*$ also. Once normalized, the statistics do not vary in time and convergence is improved by averaging fields in time also.

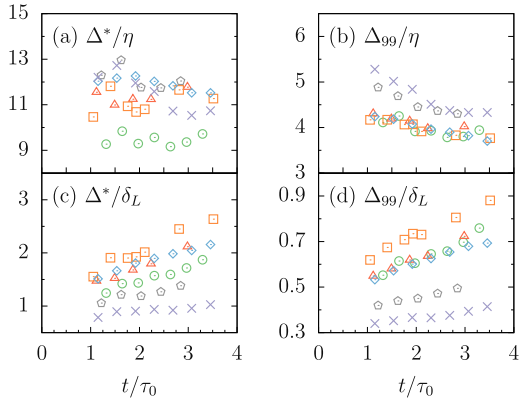

Fig. 8. Inner fractal cutoff scale Δ^* and dissipative threshold scale Δ_{99} scaled by (a-b) η and (c-d) δ_L. Symbols as in Fig. 6.

large variations in Re_λ are required to elicit significant changes in Δ^*/η. For example, a variation in Δ^*/η by a factor of 2 requires a variation in Re_λ by ≈ 7 and in $\mathrm{Re} = u'l/\nu$ by ≈ 50, which is challenging to realize in experiments and simulations alike.

It is well known that turbulence parameters differ at locations ahead and behind flames on the account of the increase in temperature. A reasonable question is whether the results shown in Fig. 5 are a manifestation of these changes. Fig. 7 shows relevant statistics for all flames at radial locations and at the flame surface via conditioning on $C = c^*$. The quantities are normalized by their values in the reactants, which have been used thusfar for scaling purposes. The nearly perfect collapse of all normalized variables demonstrates that the variation of turbulence statistics across the brush is identical for all flames. Consequently, alternative choices of reference scales at other flame locations would not change the exponent of the power law scaling Δ^*/l in Fig. 5.

Fig. 8 shows both Δ^* and Δ_{99} normalized by the Kolmogorov scale η and the laminar flame thermal thickness δ_L. Fig. 8a shows that Δ^*/η is not constant, rather displays trends consistent with Δ^*/η increasing across cases with increasing Reynolds number. Instead, Δ_{99} shows a convincing collapse with η, *independent* of Re_λ, with a minor dependence on Ka and a minor dependence on time t/τ_0 (Fig. 8b). This observation is supported by the fact that Δ_{99}/η is identical for R1K1, R2K1, and R3K1, which share the same Ka, but have different Re_λ.

We note that Δ_{99} is analogous to the dissipative threshold scale defined by Chatakonda et al. [5] (defined by the authors for 95% of the area), which was reported to be $\approx 3\eta$ and constant in high Damköhler number hydrogen/air turbulent premixed flames. Our analysis, which confirms the conclusions in Ref. [5], suggests that Δ_{99}, not the inner fractal cutoff scale Δ^*, acts as a dissipative scale for the fractal morphology of turbulent premixed flames.

These results allow us to attribute to the dissipative threshold scale Δ_{99}, defined as the scale such that $A_\Delta(\Delta_{99})/A = 0.99$, a dissipative role in the fractal behavior of the flame surface, closely related to the role of η in the velocity spectrum. When Ka changes at constant Re_λ (R3K1, R3K2, and R3K3), Δ_{99}/η shows a minor increase (Fig. 8b), consistent with the notion that flames with a larger thermal thickness push the flame's smallest wrinkles towards larger measurement scales.

Finally, both Δ^*/δ_L and Δ_{99}/δ_L (Fig. 8c and Fig. 8d) show variations over a factor of 3 across simulations and in time, indicating that neither Δ^* nor Δ_{99} are likely to be scaled by δ_L alone, at least for the flame configurations considered. We remark that the thermal flame thickness remains approximately constant at all times and in all flames.

5. Conclusions

An analysis of the fractal morphology of spherically turbulent premixed flames expanding into decaying turbulence is conducted leveraging several large-scale direct numerical simulations at varying Reynolds and Karlovitz numbers. The flames belong to the flamelet regime of turbulent premixed combustion.

Following an initial transient, the fractal dimension grows to asymptotic values between 2.3 and 2.4, depending on the Reynolds and Karlovitz numbers. The dependence of the fractal dimension on these dimensionless groups is likely due to the

Please cite this article as: T. Kulkarni and F. Bisetti, Surface morphology and inner fractal cutoff scale of spherical turbulent premixed flames in decaying isotropic turbulence, Proceedings of the Combustion Institute, https://doi.org/10.1016/j.proci.2020.06.117

narrow inertial and fractal ranges and not a fundamental property. The ratio between the inner cutoff scale and the integral length scale of turbulence exhibits a dependence on the instantaneous Reynolds number with an exponent equal to 1.14, placing the cutoff scale between the Taylor and the Kolmogorov scales. This result holds for a broad range of values of the Karlovitz number. Thus, our data suggest that the inner cutoff scale is not equal to a multiple of the Kolmogorov scale, independent of the Reynolds number. Confirming recent results by others in the literature, a true dissipative threshold scale for the surface's morphology is defined and shown to be a multiple of the Kolmogorov scale, regardless of Reynolds number.

If shown to be general and confirmed over a broader range of configurations and dimensionless groups, the Reynolds number in particular, our results may have important implications for fractal closures in turbulent premixed combustion, in that they suggest a model for the inner fractal cutoff scale and point to the fact that the transition from fractal to smooth surface morphology may occur over a range of measurement scales that widens with increasing Reynolds number.

Declaration of Competing Interest

The authors do not have any competing interest to declare.

Acknowledgments

The authors are sponsored in part by NSF grant #1805921. Numerical simulations were carried out on the "Shaheen" supercomputer at King Abdullah University of Science and Technology and on the "Stampede2" supercomputer at the Texas Advanced Computing Center with allocation TG-CTS180002 under the Extreme Science and Engineering Discovery Environment.

References

[1] F.C. Gouldin, *Combust. Flame* 68 (1987) 249–266.
[2] A.R. Kerstein, *Combust. Theor. Model.* 60 (1988) 441–445.
[3] K.R. Sreenivasan, R. Ramshankar, C. Meneveau, *Proc. R. Soc. Lond. A* 421 (1989) 79–108.
[4] F. Charlette, C. Meneveau, D. Veynante, *Combust. Flame* 131 (2002) 159–180.
[5] O. Chatakonda, E.R. Hawkes, A.J. Aspden, A.R. Kerstein, H. Kolla, J.H. Chen, *Combust. Flame* 160 (2013) 2422–2433.
[6] Y. Shim, S. Tanaka, M. Tanahashi, T. Miyauchi, *Proc. Combust. Inst.* 33 (2011) 1455–1462.
[7] T. Poinsot, D. Veynante, *Theoretical and Numerical Combustion*, 3rd, CERFACS, Toulouse, France, 2012.
[8] T. Kulkarni, R. Buttay, M.H. Kasbaoui, A. Attili, F. Bisetti, *J. Fluid Mech.* (2020). Under review
[9] S. Luca, A. Attili, E. Lo Schiavo, F. Creta, F. Bisetti, *Proc. Combust. Inst.* 37 (2018) 2451–2459.
[10] S. Luca, A.N. Al-Khateeb, A. Attili, F. Bisetti, *J. Propul. Power* 34 (2018) 153–160.
[11] O. Desjardins, G. Blanquart, G. Balarac, H. Pitsch, *J. Comput. Phys.* 227 (2008) 7125–7159.
[12] T. Kulkarni, F. Bisetti, *Proc. Combust. Inst.* 38 (2021). Under review
[13] W.E. Lorensen, H.E. Cline, *ACM SIGGRAPH Comput. Graph.* 21 (1987) 163–169.
[14] K. Falconer, Fractal geometry: mathematical foundations and applications, 2003,
[15] C.M. de Silva, J. Philip, K. Chauhan, C. Meneveau, I. Marusic, *Phys. Rev. Lett.* 111 (2013).
[16] W.L. Roberts, J.F. Driscoll, M.C. Drake, L.P. Goss, *Combust. Flame* 94 (1993) 58–62.

Please cite this article as: T. Kulkarni and F. Bisetti, Surface morphology and inner fractal cutoff scale of spherical turbulent premixed flames in decaying isotropic turbulence, Proceedings of the Combustion Institute, https://doi.org/10.1016/j.proci.2020.06.117